

Elementary acts of crystallization in an environment with high supersaturation

I. V. Melikhov

Department of Chemistry, M. V. Lomonosov Moscow State University,
Leninskie Gory, 119899 Moscow, Russian Federation.
Fax: +7 (095) 939 0126

A whole complex of phenomena occurring upon crystallization of substances from solutions and vapors has been considered. A generalized conception of crystallization has been developed. According to this conception the kinetics of the process and the properties of the crystallization product are determined not only by nucleation and molecular growth of crystals, but also by their directed aggregation. The role of the thermal and hydrodynamic selection of regular shaped aggregates in the course of their transformation into pseudo single crystals has been discussed. A relation between the properties of the crystals and their reactivity has been found.

Key words: crystallization, reactivity, clusters, aggregation, molecular growth of crystals, morphological selection, pseudo single crystals.

Crystallization is one of the most widespread processes. More than 200,000 substances are crystallized in industry around the world daily, and more than 10,000 articles are dedicated to the subject every year. However, until recently, the conditions under which crystalline substances are produced have differed only, slightly from the most ancient recipes, while crystallization concepts have been revised every 20 years.¹ The reason for this lies in the fact that each of the 145 million substances known to mankind is crystallized in such a unique way, that bringing out the general regularities of the crystallization process has been a most difficult problem.²

Currently, crystallization is represented as a combination of five processes, namely: nucleation of crystals, their molecular growth, their motion in a "collective" of particles, the formation of aggregates, and the disintegration of growing crystals upon collisions. Some of these processes have been studied in detail, but this does not enable one to describe crystallization as a whole. Therefore, there arise assumptions concerning the different impacts of the above processes on the crystallization kinetics. According to the most commonly accepted scheme, crystallization is predominantly affected by nucleation and the molecular growth of crystals, while the state of the crystals is fully characterized by their bulk.³ However, this conception, which can be called the "nucleation-growth" concept, disagrees with available data on crystallization from highly supersaturated environments.

Stages of crystallization

Usually, crystallization occurs in the liquid or gas phase where the molecules of crystallizing matter (crystallizant) are initially far apart and often dissociated into ions. In such an environment, crystallization begins when the molecules (ions) become bound into clusters. The clusters enlarge through binding of separate molecules (molecular growth) and merging of clusters (aggregate growth). Compact clusters consisting of more than 50–100 molecules can be considered as solid phase particles. They can enlarge continuously and have their own solubility.^{4,5} For instance, the solubility in an aqueous solution of $\alpha(L)$ particles of CaF_2 containing over 50 molecules (Table 1) is described by the Gibbs–Thomson–Tolman formula

$$\alpha(L) = \alpha_\infty \exp \left[\frac{2 \sigma_\infty V_M}{R T (L_0 + L)} \right], \quad (1)$$

where L is the radius of a sphere whose volume equals that of the particle; α_∞ is the thermodynamic activity of CaF_2 in a solution saturated with respect to large equilibrium form crystals; $\sigma_\infty = 0.33 \text{ J m}^{-2}$ is the surface energy of these crystals; V_M is the molar volume of CaF_2 in the solid phase; R is the gas constant; T is the absolute temperature; and $L_0 = 0.3 \text{ nm}$ is an empirical parameter. According to Eq. (1) clusters of 50 or more

Table 1. Solubility of CaF_2 clusters in a NaCl solution at 293 K*

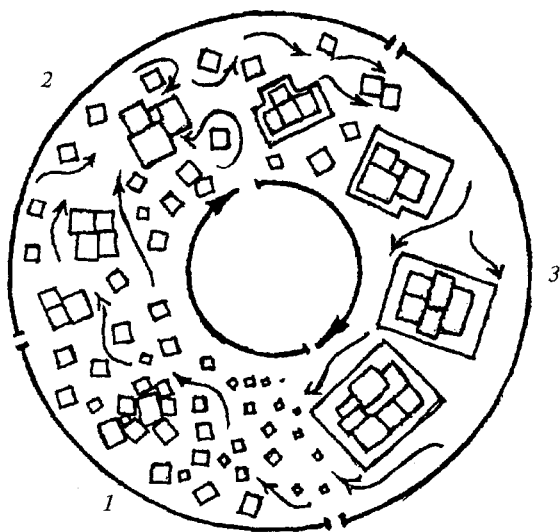
Number of molecules in the cluster	L/nm	$\alpha(L)/\alpha_\infty$
83 ± 20	0.93 ± 0.08	180 ± 8
180 ± 40	1.2 ± 0.1	110 ± 5
500 ± 50	1.7 ± 0.15	35 ± 5
820 ± 80	2.0 ± 0.12	10 ± 3

* See Ref. 5.

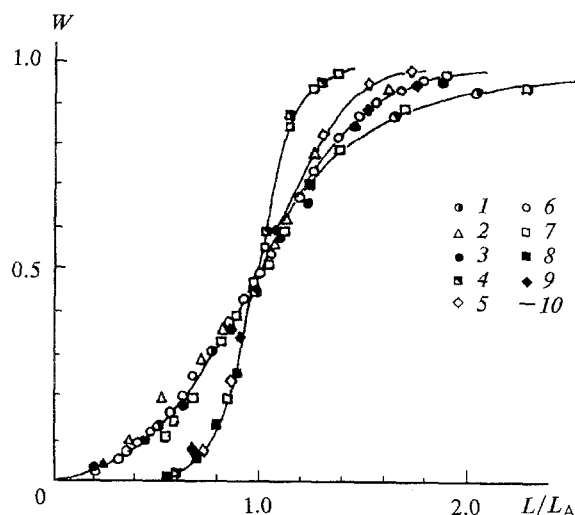
CaF_2 molecules can be characterized by the surface energy $\sigma = \sigma_\infty L(L_0 + L)^{-1}$. The σ_∞ value for electrolyte crystals in aqueous solutions is known to be related to α_∞ (see Ref. 6). Using these relationships and Eq. (1) one can estimate $\alpha(L)$ for any electrolyte.

During the crystallization process the number and size of the solid phase particles gradually increase. This leads to a decrease in the crystallizant concentration in the environment, while the rate of aggregate growth increases. As a result, crystallization becomes a three stages process: it begins with the molecular growth stage, it passes through the aggregate-molecular growth stage, and is completed by recrystallization (Fig. 1).

As was shown by direct observations of the solid particles at the first stage,^{5,7-14} all compact particles consisting of 50 and more molecules should be consid-

**Fig. 1.** Schematic diagram of changes in the shapes of solid phase particles on crystallization from highly supersaturated solutions:

- 1, the molecular growth stage;
- 2, the period of the formation of conglomerates;
- 3, the period of the coating of conglomerates.

**Fig. 2.** Size distribution of the solid phase particles at the end

of the first $W = V \int_0^L \phi dL$ (1-5) and the second stage

$$W = V \int_0^{L_1} \phi dL_1 \quad (6-9)$$

1, $\text{CaSO}_4 \cdot 0.5\text{H}_2\text{O}$, $L_A = 30$ nm; 2, $\text{Fe}(\text{OH})_3$, $L_A = 1.5$ nm; 3, $\text{Ca}_3(\text{PO}_4)_2$, $L_A = 23.8$ nm; 4, CaF_2 , $L_A = 3$ nm; 5, BaSO_4 , $L_A = 2.5$ nm; 6, $\text{CaSO}_4 \cdot 0.5\text{H}_2\text{O}$, $L_A = 44$ nm; 7, $\text{Zn}(\text{C}_2\text{O}_4)_2$, $L_A = 0.2$ nm; 8, CaF_2 , $L_A = 17.5$ nm; 9, BaSO_4 , $L_A = 30$ nm; 10, solved using (2)-(6).

ered as continuously growing spheres; their state can be described by the distribution function $\phi(L, t) = \delta N(t)/\delta L$, where $N(t)$ is the number of particles smaller than L in a volume unit at the moment t (Fig. 2). The change in the state of the particles during the first stage is in agreement with the Fokker-Plank equation

$$-\frac{\delta \phi}{\delta \tau} = \frac{\delta}{\delta L} \left[G\phi - \frac{\delta}{\delta L} (D\phi) \right] \text{ at } \left[G\phi - \frac{\delta}{\delta L} (D\phi) \right]_{L \rightarrow 0} = J, \quad (2)$$

$$G = (\omega_+ - \omega_-)l \quad \text{and} \quad D = 1/2 (\omega_+ + \omega_-)l^2,$$

where G is the growth rate; D is the fluctuation coefficient; ω_+ and ω_- are the average frequencies of attachment and detachment of molecules to and from the particle, respectively; J is the frequency of the appearance of particles (the nucleation rate) which can grow continuously with the rate G . There is little reliable data on J and G rates. Usually, the frequency J is determined by the change in the number of crystals at the late stages of crystallization, while the growth rate is determined

Table 2. The kinetics parameters of the first stage of crystallization from an aqueous solution

Crystallizant	<i>T</i> /K	<i>X</i>	$q\omega_0/\text{m}^{-2} \text{ s}^{-1}$	$J_0/\text{m}^{-3} \text{ s}^{-1}$	<i>m</i>	References
NaCl	298	$9.87 \cdot 10^{-2}$	$(2.3 \pm 0.2) \cdot 10^{23}$	—	—	3
CaSO ₄ · 0.5H ₂ O	363	$2.91 \cdot 10^{-4}$	$(3.4 \pm 0.3) \cdot 10^{19}$	$1.7 \cdot 10^{17}$	1.5	10
CaF ₂	293	$3.96 \cdot 10^{-6}$	$(1.7 \pm 0.2) \cdot 10^{13}$	$5 \cdot 10^{15}$	1.0	5
BaCO ₃	298	$2.74 \cdot 10^{-6}$	$(7.7 \pm 0.6) \cdot 10^{16}$	$1.4 \cdot 10^{17}$	1.5	9
BaSO ₄	298	$1.87 \cdot 10^{-7}$	$(1.0 \pm 0.08) \cdot 10^{15}$	$5 \cdot 10^{14}$	1.5	9
Fe(OH) ₃	298	$7.9 \cdot 10^{-12}$	$(6.2 \pm 1.2) \cdot 10^{-7}$	$1 \cdot 10^{-66}$	4.0	11

from the behavior of large crystals; however, the obtained estimates are only roughly approximate. A direct observation of nano- and microparticles for a number of substances^{7,10,14} results in the formula

$$J = J_0 \left(\frac{\alpha}{\alpha_\infty} \right)^m, \quad (3)$$

where J_0 and m are the kinetics coefficient and the order of the nucleation process, respectively (Table 2), α is the thermodynamic activity of the crystallizant in the environment. As can be seen from formula (3), the behavior of all clusters with fewer than m molecules can be characterized by only one parameter, J_0 . However, one should ascribe a considerably slower rate of enlargement to the clusters containing m molecules than to the rest of the clusters. Clusters of m molecules likely have a configuration that causes binding one molecule to enable the rapid binding of successive molecules.

Information on the growth of solid phase particles^{5–15} can be summarized by the relations

$$\omega_+ = 4\pi L^2 \omega_0 \alpha / \alpha_\infty, \quad \omega_- = 4\pi L^2 \omega_0 \alpha(L) / \alpha_\infty, \quad (4)$$

$$l = V_M q (4\pi L^2)^{-1},$$

where ω_0 is the characteristic frequency of binding of molecules to a particle, q is the cooperativity factor of the growth of particles, V_M is the molecular volume.

As was shown experimentally, the molecules join unafaceted particles independently of one another, so that $q \rightarrow 1$. When particles have faces, the transfer of a molecule to another face can cause an avalanche of transfers of other molecules until the formation of a monolayer on that face or on the whole surface, so that $q \rightarrow 4\pi L^2 V_M^{-2/3}$. In that case the particles grow layer by layer, which was confirmed by direct observation of the appearance of layers, as well as on the shape of the particles and q values.^{3,5,15}

If the crystallizant is dissociated, the frequencies of the binding of ions with opposite charges differ initially, which results in charging of particles relative to the environment (the growth charging). The charge slows down the binding of like ions and promotes the binding

of counterions. As a result, the frequencies ω_\pm for unlike ions are gradually equalized and the latter begin passing synchronously to the surface of particles, as in molecules. The charge of the particles disappears at the rate of ions migration in the body of the solid phase. These phenomena, experimentally studied in detail, have also been analyzed theoretically.¹⁵ Frequencies J_0 and ω_0 for the crystallization of dissociating substances from an aqueous solution, computed using observations of particles of size 1–100 nm, are listed in Table 2. With a fairly high accuracy they satisfy the formula

$$\omega_0 q = B X^{\alpha n}, \quad (5)$$

where $B = 2.0 \cdot 10^{24} \text{ M}^{-2} \text{ s}^{-1}$; X is the molar fraction of crystallizant in a saturated solution in pure solvent; $\alpha = 0.685 \pm 0.005$; n is the number of ions into which a crystallizant molecule dissociates.

Analyzing formulas (4 and 5) one can follow the change in the main characteristics of the first stage of crystallization for all substances under study, the $\phi(L, t)$ function. Relationship (5) makes it possible to calculate $\phi(L, t)$ for all electrolytes. However, to develop this method one must know the $J_0(\alpha, T)$ function, which has not been found yet, possibly due to the effect of random factors. The role of one of these factors, small quantities of impurities, was established in a study of the crystallization of Ca₃(PO₄)₂.¹⁰

The second stage of crystallization was studied by "screening" using optical and electron microscopy, isotope exchange, laser grading, chemical etching, and cathodoluminescence decoration for all substances listed in Table 3. At that stage the formation of microcrystalline aggregates dominates, while a parallel molecular growth continues. Even in the first stage microcrystals join one another to form disordered floccules, in which the microcrystals continue growing almost in the same way as outside the floccules. At the end of the first stage, ordered aggregates, in which the microcrystals are strictly ordered with respect to one another and joined by crystalline "bridges" are formed outside and inside the floccules. Such aggregates (conglomerates) are rather rare and enlarge by binding discrete microcrystals.^{5,7–14} In highly supersaturated environments a lot of conglomerates accumulate as late as outset of the second stage.

Table 3. Parameters of the aggregate growth at the end of the second crystallization stage

Crystallizant	S_0	m_1	$\bar{V} \cdot 10^{26}/\text{m}^3$	$\bar{L}_1 \cdot 10^8/\text{m}$	$D/G/\text{nm}$
$\text{CaSO}_4 \cdot 0.5\text{H}_2\text{O}$	2.6	0	$7.3 \cdot 10^4$	280.0	$(8.0 \pm 0.4) \cdot 10^3$
CaF_2	$3.6 \cdot 10^2$	0.5	2.7	1.7	0.2 ± 0.02
CaF_2	$8.9 \cdot 10^3$	0.5	6.4	3.5	0.5 ± 0.05
BaCO_3	$1.2 \cdot 10^4$	4.0	6.5	7.0	2.1 ± 0.1
FeOOH	$3.7 \cdot 10^{21}$	5.0	3.4	7.0	34.0 ± 2

They become so large that each one can be considered as a continually increasing polyhedron and their aggregation can be characterized by the distribution function $\varphi(L_1, t) = \delta N_A(t) / \delta L_1$, where $N_A(t)$ is the number of conglomerates smaller than L_1 per unit volume of solution; L_1 is the length of a polyhedron edge taken as characteristic. The change in the conglomerates state at the beginning of the second stage is described by Eq. (2) when

$$G = (\Omega_+ - \Omega_-)L_{10}, D = (1/2)(\Omega_+ - \Omega_-)L_{10}^2, \\ L_{10} = \bar{V}qf^{-1}, J = J_{10}N^{m_1}, \quad (6)$$

where Ω_+ and Ω_- are the average frequencies of attachment and detachment of microcrystals to and from conglomerates; L_{10} is the increment of L_1 in a single binding, \bar{V} is the average volume of conglomerates; f is the surface of conglomerates; J_{10} is the characteristic frequency of the appearance of conglomerates built up of m_1 microcrystals; N is the number of microcrystals per unit volume not involved in conglomerates.

From the data on the formation of conglomerates listed in Table 3 and from relationship (6) it follows that in all studied cases the frequency Ω_+ is many orders of magnitude smaller than the frequency of collisions of each conglomerate with microcrystals, $\Omega_+ \approx \Omega_-$. Only a small portion of collisions results in binding of the microcrystals to the conglomerates, while most of the bound microcrystals break off later. Only those microcrystals that appear to be firmly bound to the conglomerates after many repeated failures are irreversibly built into the conglomerates.

Only a few separate microcrystals ($N \rightarrow 0$) are left in the environment at the end of the second stage, and the conglomeration process slows down. If the supersaturation of the environment is still retained until that moment, the conglomerates continue to grow covered by a crystallizant "crust" (see Fig. 1), and the change in their number is very slow.

By the beginning of the third stage the crystallizant concentration drops so drastically that the difference in the solubilities of crystals of different size becomes a determining factor. At this stage the smaller crystals are dissolved, while the rest continue growing until the complete disappearance of supersaturation.

Morphological selection of the particles of the crystallizing phase

The solid phase is characterized by a variety of shapes and sizes of particles (particularly those of aggregates) at any moment of crystallization. As a rule, the crystals differ in size by an order of magnitude and more, and there are forms with different random configurations among the aggregates.³⁻¹⁰ The number of aggregates with randomly located crystals decreases in the course of time, while the aggregates whose shapes approach that of a regular polyhedron accumulate in the system. This phenomenon, called morphological selection, is due to the following processes.

There is growing relief (dendrite aggregates, vicinal hills, steps of growth) on the surface of the growing crystals; therefore, if the crystals form aggregates, they can not approach one another to the distance of molecular contact, and there is always a gap between them, filled with solution. The electrostatic repulsion of the double electrostatic layers, which partly compensates for the molecular attraction of the crystals, also favors retention of the gap. If the crystallizant is dissociated, electrostatic repulsion operates due to the increased charging of the crystals. Because of the existence of the gap the bound crystals can slide over each others' surfaces until they separate. The separation of microcrystals results from Brownian motion, that of the large crystals — from the motion of the solution. If there is a step on the surface of one of the bound crystals, and the height of the step is commensurate with the size of that crystal, binding of the second crystal is facilitated. The second crystal after sliding over the surface of the first one, can be held back by the step and remain immobile for some time. If it remains immobile for a reasonably long time, it will adhere to the step.^{16,17} As was shown by a theoretical analysis,¹⁶ the duration of the period of immobility and the magnitude of the forces that make the crystals move and turn with respect to one another depends on the flow rate and configuration of the crystals. If the crystals are the same size and their sticking together results in a regular polyhedron, the period of immobility is maximum and the forces acting on the crystals are minimum.

We discovered morphological selection when we were crystallizing various substances from aqueous solutions,

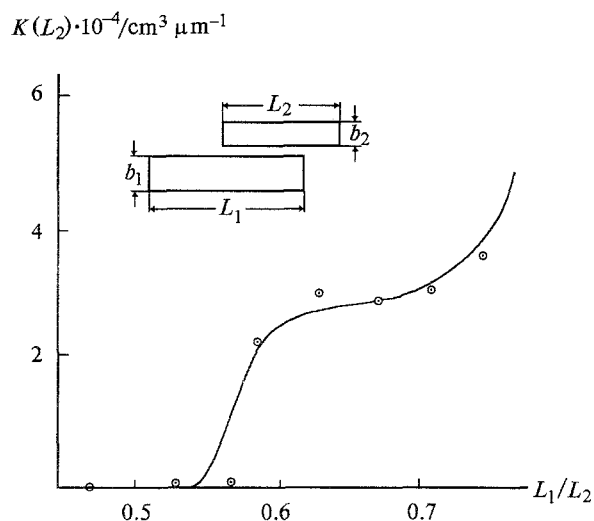


Fig. 3. The distribution coefficient of paired aggregates by sizes of the constituent microcrystals; crystallization of $\text{CaSO}_4 \cdot 0.5\text{H}_2\text{O}$ in an apparatus with a stirrer¹⁷. $T = 363 \text{ K}$; $\text{Re} = 9.4 \cdot 10^3$; $C = 0.11 \text{ mol dm}^{-3}$; $L_1 = 107 \mu$, $b_1 = 5.68 \mu$; $b_2 = 4.75 \mu$; $d = 0.71 L_2$. The radius of the stirrer $R = 1.05 \text{ cm}$; the rotation speed $\Omega = 10 \text{ s}^{-1}$; the energy dissipation $0.029 (2\pi\Omega)^3$ (dots — experiment; line — calculation).

organic liquids, and gas mixtures.^{5,9,13,17,18} Data on aggregate concentration (Fig. 3) during crystallization of $\text{CaSO}_4 \cdot 0.5\text{H}_2\text{O}$ in the turbulent flow of a phosphoric acid solution are represented by the relation

$$K(L_2) = \varphi(L_1, L_2, b_1, b_2, d) / \varphi(L_1, b_1) \varphi(L_2, b_2),$$

where $\varphi(L_1, L_2, b_1, b_2, d)$ is the function of the distribution of aggregates by the size of the microcrystals they consist of; $\varphi(L_1, b_1)$ and $\varphi(L_2, b_2)$ are functions of distribution by microcrystal size; L_1, L_2 and b_1, b_2 are the lengths of the longest and shortest edges of the first and second crystals building up the aggregate; d is the distance by which the faces of the crystals are offset from each other. The results of a $K(L_2)$ calculation carried out with the assumption that all collisions of microcrystals result in their sticking together (with the Hamaker constant $A = 2 \cdot 10^{-20} \text{ J}$ and with negligible electrostatic repulsion) are represented in Fig. 3; however each aggregate can be destroyed by turbulent pulsation through shear and rotation mechanisms.¹⁶

The calculations are in agreement with the experiment if the average gap between the crystals is $h = 60 \text{ nm}$. This is precisely the gap caused by the growth steps that were found when the aggregates were examined under a microscope. The data presented in Fig. 3 indicate that, if the growth relief is well developed, aggregates of particles of like size accumulate in the suspension. This means that in the process of aggregation selection occurs in accordance with the principle "equal joins its equal". Dramatic examples of such selection were found while studying the crystallization of

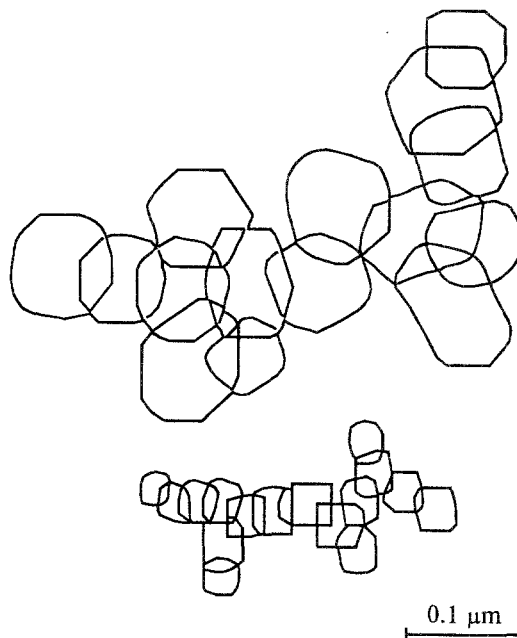


Fig. 4. Solid phase particles at the end of the first stage of crystallization of zirconium acetylacetonate¹⁸ (salting-out by heptane from a toluene solution, 293 K , $t = 11 \text{ s}$). Data of transmission electron microscopy.

zirconium acetylacetonate $\text{Zr}(\text{acac})_4$ from a toluene solution and that of BaSO_4 from an aqueous solution. The solid $\text{Zr}(\text{acac})_4$ phase was found to consist of aggregates of only small or only large microcrystals in the beginning of the aggregate-molecular growth stage (Fig. 4), and the frequency of the appearance of these aggregates was 15 orders higher than that expected for equiprobable binding of small and large particles.

Thread-like and sometimes lamellar or isometric nanocrystals are formed during crystallization of BaSO_4 from aqueous solution; at the aggregate growth stage they develop ring-shaped aggregates, and the ring-shaped aggregates merge into polyhedrons. When the polyhedrons are observed under a transmission electron microscope the rings that they consist of, can be seen. The polyhedrons bind to each other to form secondary ring aggregates. Then, the polyhedrons left outside the rings fill the space between the rings, and turn into secondary prismatic shaped polyhedrons analogous to the primary polyhedrons. The process of the mosaic-like building of the aggregates into regular polyhedrons takes place without pronounced recrystallization of the solid phase.^{9,13,17}

Information on morphological selection is scarce, since most researchers have never considered aggregate-molecular growth, and have restricted themselves to determining the number of particles of the solid phase without carrying out a morphological analysis. One can not observe a morphological selection under these con-

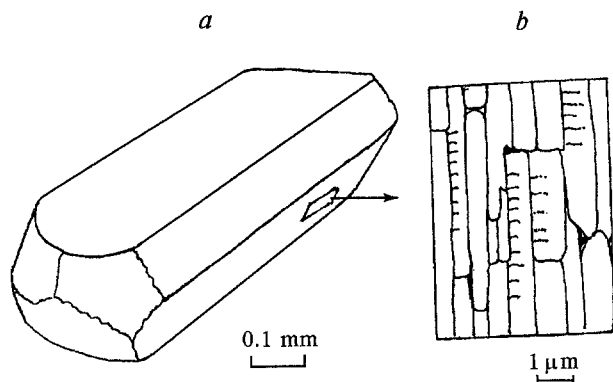


Fig. 5. Pseudo single crystals of $\text{CaSO}_4 \cdot 0.5\text{H}_2\text{O}$. Chemical crystallization from a phosphoric acid solution at 363K, the end of the second stage⁷; general view (a); the surface relief (b).

ditions. At the same time, a look at a sampling of photographs of solid phase particles showed that "the equal joins its equal" principle appeared to be true in all cases.

The mimicry of single crystals

At the second stage of crystallization the conglomerates grow to look like single crystals (Fig. 5), though the microrelief reflecting their inner heterogeneity is retained. Cleaving and etching of pseudo single crystals showed that they consist of the microcrystals that were formed during the stage of molecular growth; the microcrystals are strictly oriented with respect to one another and look somewhat larger. For instance, disorientation of the edges of the same type for the $\text{CaSO}_4 \cdot 0.5\text{H}_2\text{O}$ microcrystals does not exceed 0.05π .

The pseudo single crystals are formed as a result of the morphological selection and molecular growth of microcrystals in the aggregates. The specific character of the growth in the aggregates is due to contact of the microcrystals with one another. Most microcrystal faces, at the surface of the aggregates have edges that contact neighboring microcrystals. The "contacting" edges can be the origin of the growth steps, which promote the growth of faces. As a result, the faces with active contacting edges gradually disappear (thin out) which makes the shape of the aggregate and that of the single crystal

approach each other. The negative curvature of the areas close to the contacting edges also plays a role. The thinning out of faces in microcrystals of $\text{CaSO}_4 \cdot 0.5\text{H}_2\text{O}$ (see Ref. 7) and NH_4ClO_4 (see Ref. 19) has been observed in detail. However, thinning out was not detected in the aggregates of large $\text{CaSO}_4 \cdot 0.5\text{H}_2\text{O}$ ($L > 100\mu$) crystals.²⁰ There are many "powerful" sources for creating steps on the faces of crystals which contacting edges can not compete with. The mechanism of thinning is not entirely understood. However, if the aggregates are large and their shapes are very irregular, thinning has no chance to be completed during the second stage of crystallization. If the aggregates are small and their shapes are fairly regular due to morphological selection, thinning rapidly turns them into pseudo single crystals.

Data on the formation of pseudo single crystals during crystallization at different starting supersaturations of the environment S_0 is given in Table 4. Here N_0 is the number of microcrystals in suspension at the end of the second stage, namely, at the moment t_0 when only 5 % of all microcrystals have been incorporated into the aggregates; N_1 is the number of pseudo single crystals at the moment t_1 when their number is 95 % of all available microcrystals; P is the number of faces of a microcrystal to which the succeeding microcrystals have been bound during the formation of a pseudo single crystal. The experimental data are approximately described by the equation

$$N_1 = N_0 \exp[-0.18P^2], \quad t_1 = t_0(1 + 0.07P^2) \quad (7)$$

at any initial supersaturations and temperatures which affect N_0 and t_0 . A change from N_0 to N_1 or from t_0 to t_1 is mostly determined by geometric factors (through parameter P).

As has been shown by detailed studies^{13,21,22} pseudo single crystals can grow together stage by stage at $t > t_1$ to form pseudo single crystals in the second and later generations. The growth stages follow one another until the aggregates reach the size at which they precipitate to the bottom of the crystallizer, and morphological selection comes to an end. If crystallization lasts a sufficiently long time, the solid phase develops a multilayer hierarchy texture consisting of the last generation pseudo single crystals built up of the grown together pseudo single crystals of the preceding generation, etc. The solid phase forms a new layer of its texture at each stage.

Table 4. Parameters of formation of pseudo single crystals

Crystallizant	S_0	T/K	t_0/s	t_1/s	N_0/m^{-3}	N_1/m^{-3}	P
BaCO_3	$1.2 \cdot 10^4$	298	0.5	—	$3.4 \cdot 10^{21}$	$5.0 \cdot 10^{17}$	7
BaSO_4	10^3	298	0.2	0.6	$3.0 \cdot 10^{15}$	$5.0 \cdot 10^{13}$	5
CaF_2	$8.9 \cdot 10^3$	293	—	—	$8.4 \cdot 10^{20}$	$2.8 \cdot 10^{18}$	6
$\text{ZnC}_2\text{O}_4 \cdot 2\text{H}_2\text{O}$	20.0	298	300.0	$1.2 \cdot 10^3$	$>10^{19}$	$1.0 \cdot 10^{17}$	7
$\text{CaSO}_4 \cdot 0.5\text{H}_2\text{O}$	2.6	353	6.0	30	$2.0 \cdot 10^{19}$	$1.5 \cdot 10^{14}$	8
NaCl	1.08	298	60.0	200	—	$1.6 \cdot 10^{10}$	6

The tendency for aggregates to form into pseudo single crystals, which we called single crystal mimicry, is one of the self-organizing forms of a crystallizing phase. A phase consisting of ultramicrocrystals is ordered due to Brownian motion, while a low disperse phase is ordered due to the motion of the solution. And though fluxes of heat and mechanical energy are not ordering factors, the solid phase is self-organized through the mechanism of morphological selection. No doubt, ordering of this type is temporary. The pseudo single crystals are recrystallized into genuine single crystals at the third stage of crystallization. However the life time of pseudo single crystals can be indefinitely long. All things considered, one can expect the development of a new direction in synthetic chemistry — the directed synthesis of pseudo single crystals with deliberately constructed inner structures.

The reactivity of the solid phase

The reactivity of the solid phase changes sharply in the process of crystallization. If the solid phase is represented as the sum of a number of structural elements (perfect areas of faces of diverse types, dislocations coming to the surface, boundaries of grown together crystals), the reactivity can be characterized by the sum of the contributions of all of the structural elements to the specific rate of a reaction proceeding under standard conditions. In the reaction of the crystallizant with a standard reagent B $A_{solid} + B \rightarrow AB$ this sum is equal

$$Z(\tau) = (M\alpha_A\alpha_B)^{-1} \sum_j \frac{dM_j}{d\tau}, \quad (8)$$

where M is the number of moles of crystallizant at reaction time τ ; α_A and α_B are the thermodynamic activities of the crystallizant and reagent B under standard conditions in the reaction environment; M_j is the number of moles of crystallizant in the j -th structural element.

The molecules forming each structural element can be in different states,

$$\frac{dM_j}{d\tau} = M_j \int_0^\infty \omega \phi_j(\omega) d\omega \quad \text{at} \quad M_j = 4\pi \int_0^\infty \Phi_j L^2 \varphi(L, t) dL, \quad (9)$$

where $\phi_j(\omega)$ is the density distribution of molecules of the j -th element by frequency ω of participation in the reaction, Φ_j is the molar content of crystallizant on the j -th element per unit of surface. According to formulas (8) and (9) a change in $Z(\tau)$ during the process of crystallization is due to changes in $\phi_j(\omega)$, Φ_j and $\varphi(L, t)$.

In the general case, the $\phi_j(\omega)$ functions are unknown. For BaCO_3 they can be determined from experimental data¹³ from the changes in the relief of the surfaces of the particles during the short time they are in contact with the sodium ethylenediamine tetraacetate solution (Fig. 6). If sodium ethylenediamine tetraacetate is assumed to be the reference reagent, and the local shift of each surface area of the BaCO_3 particles during their contact with the solution is proportional to ω , then after measuring the local shifts on the electron microscopy diagrams of the crystals¹³ one can obtain the relation

$$W_j = \int_0^\omega \phi_j(\omega) d\omega = 1 - \exp\left[-0.5\left(\frac{\omega}{\bar{\omega}_j}\right)^4\right], \quad (10)$$

where W_j is the portion of the j -th element whose reacting frequency is smaller than ω ; $\bar{\omega}_j$ is the characteristic frequency of participation in the reaction for the molecules of the j -th element.

For the faces of the BaCO_3 pseudo single crystals $\bar{\omega}_j$ was measured to be 430 s^{-1} ; for the boundaries of the grown together particles of the previous generation coming to the surface of the pseudo single crystals $\bar{\omega}_j$ was 10^3 s^{-1} . Thus, the reacting of BaCO_3 on the faces of crystals differs from that on their fused surfaces by a factor of approximately 2.

If by analogy with BaCO_3 one assumes that all structural elements of any solid face possess the same

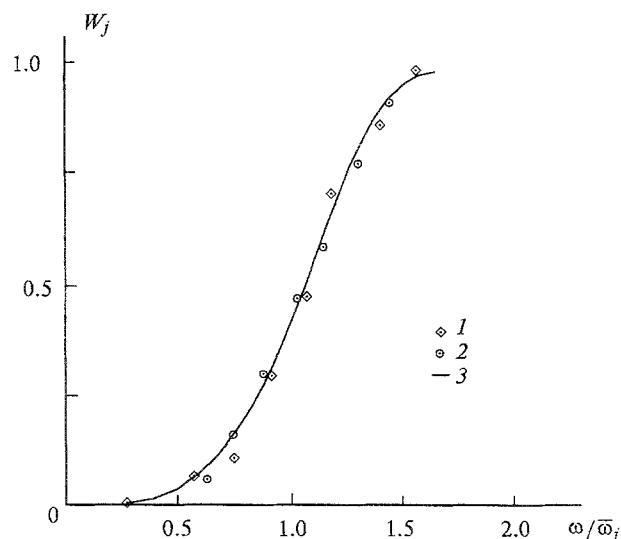


Fig. 6. Distribution of the "molecules" of the BaCO_3 solid phase by frequency of interaction with a solution of sodium ethylene diamine tetraacetate. Crystallization from a solution with initial supersaturation $S_0 = 1.2 \cdot 10^4$, 298 K, $t = 62.5 \text{ s}$, $\tau = 3 \text{ s}$:

- 1, crystallizant on the crystals faces;
- 2, on microcrystallite boundaries;
- 3, calculations using formula (10).

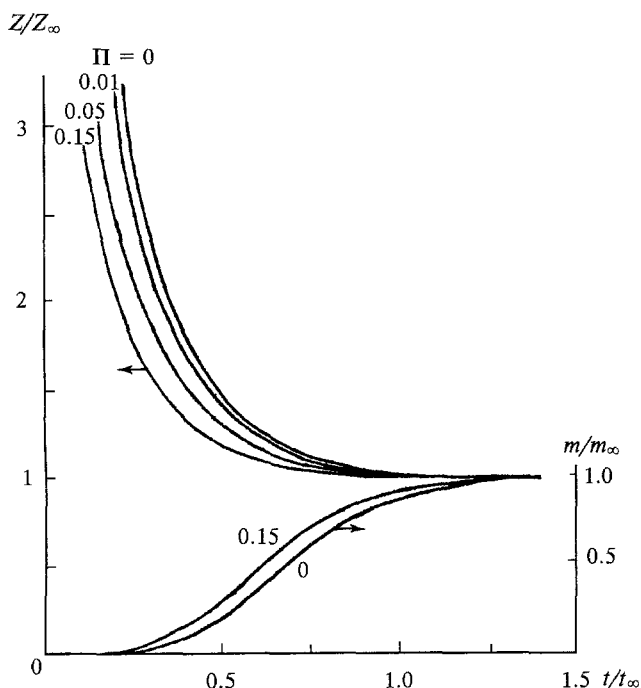


Fig. 7. Changes in the reactivity and the solid phase mass in the course of crystallization in a closed system.

functions $\phi_j(\omega)$, which do not change in the course of crystallization, then, solving Eqs (1)–(10) one can find $Z(t)$. Figure 7 shows the solutions of these equations for crystallization in a closed system in which the activity coefficient of crystallizant in solution is constant and the parameter

$$\Pi = V_M q(a_0 + a_\infty) \cdot [8\pi E^3(a_0 - a_\infty)]^{-1},$$

where $E = 0.7[BA_0^2 M_0 S_0 J_0^{-1} X^{1+2.05n}]^{1/4}$; A is Avogadro's number; $S_0 = (a_0 - a_\infty)/a_\infty$ is the initial supersaturation of the solution; M_0 is the number of moles per unit volume of the saturated solution of crystallizant is variable. The values of $Z(t)$ are referred to the reactivity of the final solid phase Z_∞ ; time t is referred to the characteristic time t_∞ of precipitation of the overwhelming bulk (m) of the solid phase

$$t_\infty = 1.4 \left[\frac{AM_0 X^{1-2n}}{J_0 B_3 V_M^2 S_0^3} \right]^{1/4}.$$

As can be seen, the reactivity of the solid phase decreases by more than a factor of 3 upon precipitation of a half of the final bulk m_∞ for the whole interval of possible changes in the number Π . A hypothetical phase whose reactivity does not depend on the number of point defects in the crystals is characterized in Fig. 7. If the defects accelerate the reaction, the $Z(t)$ depend-

ence is sharper, since the disorder in crystals decreases in the course of crystallization²³.

The generalized conception of crystallization

Judging from information on different types of crystallizants, the crystallization kinetics and the properties of the final solid phase are determined by nucleation, the molecular growth of crystals and the multi stage aggregate-molecular growth of particles. The formation of pseudo single crystals with a multilayer hierarchical texture is the most important trend in long-term crystallization in a mobile environment. A complete picture of crystallization can be revealed only through a long-term observation of the process. One should begin the observations at the moment of supersaturation of the environment and finish them at the moment when the particles are enlarged to such an extent that they precipitate to the bottom of the crystallizer. Short term monitoring gives rise to uncertainty in the interpretation of the data. Usually, the interval between observations is increased until one can understand whether eq. (2) is applicable and one can determine G , D and J . However, one can use that equation both for the molecular growth stage (4) and for the aggregate-molecular growth stage (5), which makes the results of the determination ambiguous. Were it not for single crystal mimicry, one could differentiate the molecular growth stage from the aggregate stage by the shape of the solid phase particles: at the stage of molecular growth they would have a regular shape, while at the stage of aggregate growth their shape would be irregular. However, the fact that pseudo single crystals form makes this criterion inapplicable.

Since the aggregate growth sharply changes the properties of the solid phase, one can but rarely characterize the particle by its mass or equivalent size, as is accepted currently when describing crystallization.^{1,3,24,25} If one represents solid state particles merely as mass carriers, such properties as reactivity and catalytic activity will be ignored. For a full description of crystallization it is necessary to characterize each particle of the solid phase by the number, shape, orientation, and presence of defects of all constituent crystals, that is, one must find a many-dimensional function for the distribution of particles by states, instead of the $\phi(L,t)$ function. The determination of such a function is a difficult problem. However, without its solution, one can hardly expect the progress in crystallization research required by the vast use of this phenomenon in practice.

References

1. *Industrial Crystallization* 84, Eds. S. J. Janic and E. J. de Jong, Elsevier, Amsterdam 1984, 498.

2. G. G. Pimentel, *Opportunities in Chemistry*, Acad. Press, Washington, 1985 p.4
3. I. V. Melikhov, *Khimicheskaya promyshlennost* [Chemical Industry], 1993, 349 (in Russian).
4. Yu. M. Petrov, *Klastery i malye chastitsy* [Clusters and Small Particles], Nauka, Moscow, 1986, p. 30 (in Russian).
5. I. V. Melikhov, V. F. Komarov, and Yu. A. Kozel, *Kolloidn. Zh.*, 1991, **53**, 515 [*Colloid. J. USSR*, 1991, **53** (Engl. Transl.)].
6. J. Nyvit, O. Sohnel, M. Matuchova, and M. Broul, *The Kinetics of Industrial Crystallization*, Elsevier, Amsterdam, 1985.
7. I. V. Melikhov, I. E. Mikheeva, and V. N. Rudin, *Kristallografiya*, 1989, **34**, 1272 [*Sov. Phys.-Crystallogr.*, 1989, **34** (Engl. Transl.)].
8. I. V. Melikhov, E. D. Kozlovskaya, L. B. Berliner, and M. A. Prokofiev, *J. Colloid. Interface Sci.*, 1987, **117**, 1
9. I. V. Melikhov, A. S. Kelebeev, and S. Basis, *J. Colloid. Interface Sci.*, 1986, **112**, 54
10. I. V. Melikhov, S. Lazis, and Z. Vukovis, *J. Colloid. Interface Sci.*, 1989, **127**, 317.
11. I. V. Melikhov and E. D. Kozlovskaya, *Kolloidn. Zh.*, 1987, **49**, 180 [*Colloid. J. USSR*, 1987, **49** (Engl. Transl.)].
12. I. V. Melikhov, B. Nazirmadov, and V. F. Komarov, *Kolloidn. Zh.*, 1986, **48**, 68 [*Colloid. J. USSR*, 1986, **48** (Engl. Transl.)].
13. I. V. Melikhov, Z. Vukovis, S. Basis, and S. Lazis, *J. Chem. Soc., Faraday Trans., 1*, 1985, **81**, 1275
14. I. V. Melikhov, V. F. Komarov, and Yu. A. Kozel, *Kolloidn. Zh.*, 1988, **50**, 690 [*Colloid. J. USSR*, 1988, **50** (Engl. Transl.)].
15. A. A. Chernov, *Sovremennaya kristallografiya* [Modern Crystallography], **3**, Nauka, 1982, Moscow (in Russian).
16. I. V. Melikhov and B. M. Dolgonosov, *Kolloidn. Zh.*, 1989, **51**, 911 [*Colloid. J. USSR*, 1989, **51** (Engl. Transl.)].
17. I. V. Melikhov, O. V. Kuleshova, B. M. Dolgonosov, and M. P. Moroz, *Kolloidn. Zh.*, 1991, **53**, 378 [*Colloid. J. USSR*, 1991, **53**, (Engl. Transl.)].
18. I. V. Melikhov, S. S. Berdonosov, and I. A. Kopylova, *Kolloidn. Zh.*, 1993, **55**, 114 [*Colloid. J. USSR*, 1993, **55** (Engl. Transl.)].
19. I. V. Melikhov, E. Ya. Khananova, and V. M. Podkopov, *Neorgan. Materialy* [Inorgan. Materials], 1992, **28**, 1537 (in Russian).
20. O. V. Kuleshova, Ph. D. Chem. Thesis, MGU, Moscow, 1991, p.129 (in Russian).
21. A. S. Kelebeev, Ph. D. Chem. Thesis, , MGU, Moscow, 1982, p.172 (in Russian).
22. P. J. Murphy, A. M. Posner, and J. P. Quirk, *J. Colloid. Interface Sci.*, 1976, **56**, 298.
23. I. V. Melikhov and Zh. Vukovich, *Zh. Fiz. Khimii*, 1972, **46**, 328 [*J. Phys. Chem.*, 1972, **46** (Engl. Transl.)].
24. O. M. Todes, V. A. Seballo, and A. D. Goltsiker, *Massovaya kristallizatsiya iz rastvorov* [Bulk Crystallization from Solutions], Khimiya, Leningrad, 1984 (in Russian).
25. Z. Rajkowski and J. Synowiec, *Krystalizacja i krystalizatory*, Naukowo-Tecniezne, Warszawa, 1991.

Received June 6, 1994